

Collisional depopulation of $\text{He}(n^1P)$ ($4 \leq n \leq 13$) in thermal collisions with $\text{He}(1^1S)$

W. R. Pendleton, Jr.,* M. Larsson, and B. Mannfors

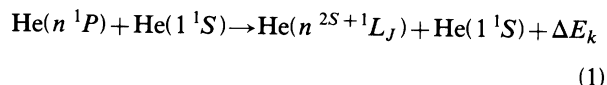
*Research Institute of Physics, S-104 05 Stockholm 50, Sweden**and Physics Department, Royal Institute of Technology, S-100 44 Stockholm 70, Sweden*

(Received 14 April 1983)

Total collisional depopulation rates for $\text{He}(n^1P)$ ($4 \leq n \leq 13$) in thermal collisions with $\text{He}(1^1S)$ have been measured using the transient-decay method. Related loss cross sections increase in proportion to n^4 in the limited range $4 \leq n \leq 6$, reach a maximum of $2600 \pm 600 \text{ \AA}^2$ at $n=10$, and decrease approximately in proportion to $n^{-2.5}$ for $11 \leq n \leq 13$. The measurements were found to be inconsistent with a strong "selection rule," $\Delta L=2$, for the $\text{He}(n^1P)$ -He collisions. A model in which ΔL for the collision is largely unrestricted provides a satisfactory interpretation of the observations, in agreement with recent l -mixing studies of atomic Rydberg levels. The experimental cross sections compare favorably with values calculated using an approximate scaling formula for collisional l mixing and, for $n > 10$, with predictions based on a simple perturbation treatment in the weak-collision approximation.

I. INTRODUCTION

The collisional transfers of $\text{He}(n^1P)$ excitation energy to other helium levels through binary-collisional processes of the type

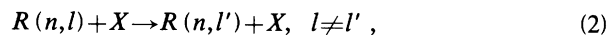


with ΔE_k the energy defect in the collision, have been studied extensively since the early work of Lees and Skinner¹ and Maurer and Wolf.^{2,3} However, significant questions remain unanswered concerning the details of the collisional processes which redistribute the n^1P excitation. These questions relate to the following: (1) the selection rule, if any, for ΔL , the change in orbital angular momentum; (2) the details of the singlet-triplet transfers which probably take place through the "gateway" states with $L \geq 3$; (3) the magnitude and n dependence of the total loss cross sections.

Previous measurements of $\text{He}(n^1P)$ collisional loss in encounters of type (1) have been reported by a number of investigators.⁴⁻¹⁵ The available results are restricted to $n \leq 7$ and exhibit a dispersion which greatly exceeds the uncertainty estimates. In addition, the dependence of the loss cross section on n over the range $4 \leq n \leq 7$ is not well established. Various investigators have reported cross sections which increase with n (approximately as n^4 for $4 \leq n \leq 7$),^{8,10} decrease with n ,¹¹ or show no clearly discernible trend.¹²

In this paper, we report the results of a study designed to provide new information relating to process (1). The total loss of $\text{He}(n^1P)$ ($4 \leq n \leq 13$) resulting from thermal collisions with $\text{He}(1^1S)$ has been investigated using the transient method, in particular the high-frequency deflection (HFD) technique.¹⁶ The results provide new insight into process (1) and span the intermediate range of n , a region of special interest to the theory of transitions between Rydberg states induced by collisions at thermal energies.

The present study is fundamentally related to recent investigations of collisional l mixing in thermal collisions of $\text{Na}(n^2D)$ and $\text{Rb}(n^2F)$ with $\text{He}(1^1S)$. It has generally been argued that the l -changing process in collisions of the type



where R is a high ($n \gg 1$) Rydberg atom and X is a collision partner, should approximate an electron-scattering problem. The basic physical model invokes a slow collision between the Rydberg electron and the scattering species X with the parent ion R^+ acting as a "spectator" during the collision. The scattering of low-energy electrons ($E_{\text{kin}} \ll 1$ a.u.) by $\text{He}(1^1S)$ has a weak dependence on energy.¹⁷ Hence, it is expected that the $R(n,l) \equiv \text{He}(n^1P)$, $\text{Na}(n^2D)$, and $\text{Rb}(n^2F)$ results should be similar when the collision velocities are equal since the energy defects are very similar in the three cases.

Experimental l -mixing results by Hugon *et al.*¹⁸ for $\text{Rb}(n^2F)$ -He collisions and those of Gallagher *et al.*¹⁹ for $\text{Na}(n^2D)$ -He collisions have been interpreted within the framework of theoretical studies which consider only the Rydberg electron-perturber interaction. Three theoretical approaches have been used: (1) a semiclassical approach carried to the first order of perturbation theory,^{20,21} (2) a quantum-theoretical approach based on close-coupling calculations for small- n and Born-approximation calculations for large n ,^{22,23} and (3) the approach of de Prunele and Pascale²⁴ in which the total-scattering cross sections of free, low-energy electrons by the perturber are required.

A feature common to these "separated-atom" models is the neglect of the Rydberg core-target interaction; the l changing is regarded as arising solely from the scattering of the Rydberg electron by the target. In addition, electron spin is neglected in these single-valence-electron theories. It has been suggested²⁵⁻²⁷ that the core-target interaction cannot always be ignored in treating l -changing thermal collisions, but in the special case of thermal $\text{Na}(nd)$ -rare-gas collisions, an estimated upper

bound $\sim 100 \text{ \AA}^2$ has been placed on the inelastic cross section due to core effects.²⁸ This upper bound is consistent with recent estimates by Matsuzawa²⁹ and is much smaller than many of the computed and measured cross sections.

We are unaware of a complete theoretical treatment of process (1), although Cohen³⁰ has developed a multistate curve-crossing model for scattering of excited He by ground-state He and has applied it to associative ionization and excitation transfer in the case of He triplets with $n=3$. Despite this limitation, it is possible to compare the experimental results with predictions based on a generalized, approximate scaling formula for computing l -mixing cross sections³¹ and with the predictions of a simplified perturbative treatment in the weak-collision approximation.³²

II. EXPERIMENT

A. Experimental method

Total collisional depopulation rates for $\text{He}(n^1P)$ were determined by studying the lifetimes of the n^1P level populations as a function of the $\text{He}(1^1S)$ concentration. The extraction of the total collisional loss rates from the lifetime data was accomplished using a simple model which adequately described the lower-pressure data. In the low-pressure region, the $\text{He}(n^1P)$ decay rates were well represented by the expression

$$A_{\text{eff}}(n^1P) = A_r(n^1P) + \Gamma(n^1P)p, \quad (3)$$

where $A_r(n^1P)$ is the total radiative transition probability for the n^1P level (sec^{-1}), $\Gamma(n^1P)$ is the total collisional loss rate coefficient ($\text{sec}^{-1}/\text{Torr}$) and p is the helium pressure (Torr). Equation (3) implies that other atomic levels do not contribute radiatively or collisionally to the population of the level under study. These important assumptions will be explored in Sec. III.

The radiative term is pressure dependent as a result of resonance trapping of the $n^1P \rightarrow 1^1S$ radiation. When the spatial distribution of the emitting atoms has relaxed to the lowest eigenmode, this term may be expressed in the form

$$A_r(n^1P) = A_1(n^1P) + g(n^1P)A(n^1P \rightarrow 1^1S), \quad (4)$$

where $A_1(n^1P)$ is the sum of the transition probabilities for decay of the n^1P level to levels other than the ground state, $A(n^1P \rightarrow 1^1S)$ is the transition probability for decay to the ground state, and $g(n^1P)$ is the escape factor for decay in the lowest eigenmode. Details relating to the treatment of the data will be given in a subsequent section; here we merely note that the radiative term in Eq. (3) can be determined with good accuracy using well-established procedures.^{8,9} Hence, the collision term is readily evaluated and the total quenching rate determined.

Average total loss cross sections $\bar{\sigma}(n^1P)$ are subsequently inferred from the measured rate constant $\Gamma(n^1P)$ using the relationship

$$\bar{\sigma}(n^1P) = \frac{\Gamma(n^1P)}{\bar{v}}, \quad (5)$$

where \bar{v} is the average relative collision velocity and $\Gamma(n^1P)$ is expressed in concentration units ($\text{cm}^3 \text{sec}^{-1}$). The assumption of a Maxwell-Boltzmann distribution for the relative velocity yields the familiar result

$$\bar{v} = (8kT/\pi\mu)^{1/2}, \quad (6)$$

where k is Boltzmann's constant, T is the absolute temperature, and μ is the reduced mass.

B. Experimental arrangement

The basic experimental technique, the HFD method for measuring atomic and molecular lifetimes, was developed in this laboratory several years ago. Principles of the technique have previously been published,¹⁶ as has a complete description of a basic HFD system.³³ For the purposes of this paper, we recall the essential features of the experiment.

Excited He atoms were produced by bombarding a $\text{He}(1^1S)$ target with periodic pulses of 20-keV electrons. The current pulses were about 30 mA in amplitude and about $\tau/5$ in duration, with τ the effective lifetime of the level under study. Helium from a high-pressure cylinder was introduced into the target chamber by means of a regulator and a variable leak valve following high-vacuum preparation of both the gas-inlet system and the target chamber. The background pressure of residual gases in the target chamber was typically less than 10^{-5} Torr. Lifetime measurements were subsequently carried out using selected pressures in the range $1 \leq p \leq 50$ mTorr. A Leybold-Heraeus IONIVAC IM 10 ionization gauge, which was compared with an MKS Instruments Model 110 capacitance manometer, was used to monitor the target pressure.

A 2-m Czerny-Turner scanning monochromator, equipped with a cooled EMI 9789 SQ photomultiplier, was used for spectral selection and detection. An effective resolution of $< 1 \text{ \AA}$ was used for the measurements. This resolution ensured the isolation of the HeI transition of interest from other helium transitions and discriminated against weak, spectrally dense background radiation produced in the interaction of the beam with the residual gas.

Decay curves were accumulated using a conventional multichannel delayed-coincidence system. The system was calibrated to an accuracy of $< 1\%$ using known delays. Repeated checks of the time calibration yielded results which were consistent to about 0.5%.

C. Experimental uncertainties

Experimental uncertainties associated with the determination of $\Gamma(n^1P)$ arise from uncertainties in $(1/\tau)$, in the pressure measurement, and in the model used to extract the collisional loss rates from the total loss rates. Uncertainties in $(1/\tau)$ stem from statistical error ($\sim 1-2\%$) and from time calibration uncertainties ($< 1\%$). Uncertainties in $(1/\tau)$ can also arise from an overly-simplified model of the decay process. Both one- and two-component reductions of the data were carried out in this study, and the best result, based on statistical criteria, was selected. In the case of a more complex de-

cay, an undetermined systematic error would be included in the best result.

The method used to extract the collisional loss rate from the observations introduces an additional source of uncertainty. It has previously been shown,^{8,19} that effective decay-rate expressions of the form given by Eq. (3) apply to the description of the fast component in the decay of reciprocally coupled levels in both the low-collision-frequency and high-collision-frequency domains. However, the two domains are, of course, connected by a nonlinear transition region of intermediate slope. The interpretation of the radiative and collision terms is significantly different in the two domains. Neglect of this effect in interpreting the data of the present study is expected to introduce an n -dependent systematic error $\sim 10\%$ in the worst cases.⁸ It was found that the collisional loss rates for the n^1P levels were closely proportional to pressure at the lower pressures of the experiment. Correlation coefficients corresponding to linear regression analyses were typically > 0.98 . Hence, no attempt was made to correct for possible nonlinearities.

The total decay rate of He(n^1P) for $n \geq 7$ was controlled by collisions at the higher pressures of the experiment. Consequently, systematic error in evaluating the radiative loss for these higher terms has significantly less impact on the final result than in the case of the lower terms where radiation plays a more prominent role. For example, the decay-rate data for the $11^1P \rightarrow 2^1S$ transition (Fig. 6) indicate that the radiative loss rate is approximately 20% of the total loss rate at a pressure of 20 mTorr. An error of 10% in estimating the radiative loss rate at this pressure would result in an error of about 2.5% in the determination of the collisional loss rate. The collisional-loss term is physically constrained to pass through $p=0$. As a result, the slope of the linear section can be evaluated with good accuracy despite the possibility of modest errors in the determination of the radiative loss rate. A subjective estimate of the possible error from this source is $\pm 10\%$ at $n=4$ decreasing to $\pm 5\%$ for $n \geq 7$.

A pressure-measurement uncertainty of $\pm 10\%$ must be combined with the other uncertainties in estimating a total uncertainty for the $\Gamma(n^1P)$ determinations. The statistical, time-calibration, and pressure-measurement uncertainties were similar for each n . However, the model uncertainties are dependent on n , and possible n -dependent systematic errors are difficult to estimate. In the final analysis, we have assigned an uncertainty of $\pm 20\%$ to the measurement at each n .

The rotational fine-structure intensity distribution in the (0,0) band of the N_2^+ first negative system ($B^2\Sigma_u^+ - X^2\Sigma_g^+$), excited with a dc beam and a low-pressure N_2 target, was used as an index of the gas temperature. This procedure results in additional uncertainty in inferring $\bar{\sigma}(n^1P)$ from $\Gamma(n^1P)$. The uncertainty in $\sigma(n^1P)$ is estimated to be less than $\pm 25\%$.

III. INTERPRETATIONAL CONSIDERATIONS

A. Cascade

Erman¹⁶ has discussed the utility of the HFD technique in assessing the importance of cascades in the decay of ex-

cited atomic and molecular levels. However, very strong collisional effects for He(n^1P) with $n \geq 4$ precluded a convenient, unambiguous assessment of cascade in the present experiment. In the single case of the 3^1P term, which is very weakly affected by collisions,¹⁰ it proved possible to assess the role of cascade. The 3^1P data were found to be predominantly single exponential under the measurement conditions. Two-component reductions consistently failed to yield a statistically significant second decay component. Hence, cascade effects were deemed unimportant for this level.

The difficulty of experimentally verifying negligible cascade effects for the $n \geq 4$ measurements prompts us to discuss the cascade problem in more detail. In this connection it is helpful to consider the shapes and magnitudes of the excitation functions for the n^1S, n^1P, n^1D levels in He. In Fig. 1 representative excitation functions for $^1S, ^1P, ^1D$ levels are presented for the case $n=6$,³⁴ but similar relative values are expected for both larger and smaller n . The figure clearly illustrates the preferential production of He(n^1P) in (e, He) collisions for impact energies > 50 eV. The use of 20-keV electrons in the present experiment ensured nearly pure n^1P excitation by the primary beam. However, it was not conveniently possible to eliminate excitation of the target atoms by slow electrons produced by beam-target and/or beam-surface interactions. Hence, weak excitation of the n^1S, n^1D levels resulted from this secondary source of electron-impact excitation.

Two additional factors contribute to the expectation that cascade into the n^1P terms was negligible under the conditions of the experiment. First, the excitation pulse widths used in the investigation were nominally $0.2\tau(n^1P)$, where $\tau(n^1P)$ is the effective lifetime of He(n^1P). Effective n^1P lifetimes were typically some-

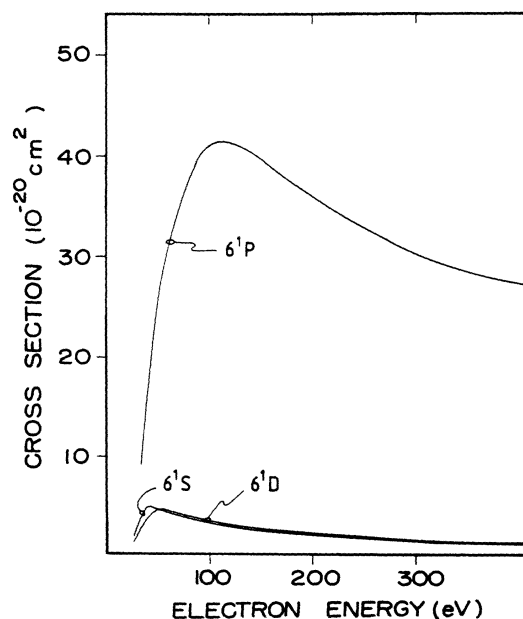


FIG. 1. Cross sections for populating the $6^1S, 6^1P, 6^1D$ levels of He by electron impact (adapted from Ref. 34).

what shorter than the radiative lifetimes of the n^1S and n^1D terms for $n \geq 7$. Thus, a short excitation period favored the growth of the directly excited $\text{He}(n^1P)$ populations. Secondly, the branching of the radiative transfers from the high- n terms favors the lower- n terms of the combining manifold. Hence, only a small fraction of the high- n excitation is passed radiatively to the high- n terms. (For example, less than 5% of the radiative transitions from the 9^1S level terminate on the 8^1P level.) In view of these considerations and the 3^1P results, it seems very unlikely that cascade effects contributed significantly in the n^1P study.

One additional piece of information which supports the premise of negligible radiative transfer to the n^1P levels of interest to this study centers around the relative intensities of the members of the series $n^1P \rightarrow 2^1S$, $n^1D \rightarrow 2^1P$, and $n^1S \rightarrow 2^1P$. Estimates of branching from the n^1S and n^1D terms to n^1P levels with $4 \leq n' < n$ consistently yielded values small compared to the observed intensity of the $n^1P \rightarrow 2^1S$ transition.

B. Resonance trapping

The n^1P levels are optically connected to the ground state and are affected by resonance-trapping effects to rather low helium pressures. The extraction of reliable collisional loss rates from the decay-rate data requires an evaluation of the radiative portion of the total effective decay rate. Hence, a quantitative treatment of resonance trapping is essential to the realization of accurate results for the collisional loss rates.

The experimental treatment of resonance trapping in helium has drawn heavily on the work of Phelps³⁵ who applied the theory of Holstein³⁶ to the problem. The key to the evaluation of resonance trapping in a given system is the determination of the effective "trapping radius," ρ_{eff} , which is characteristic of a particular collision-chamber geometry. A determination of this parameter enables one to calculate the escape factor [$g(n^1P)$ in Eq. (4)] when k_0 , the absorption coefficient at line center for a Doppler-broadened line, is known. (See the recent review by Irons³⁷ for details.)

We have determined ρ_{eff} for the collision chamber of this study by the well-established method of measuring the pressure dependence of the effective lifetime of $\text{He}(3^1P)$. Previous studies have established a total loss cross section of $\leq 3 \times 10^{-15} \text{ cm}^2$ for thermal collisions of $\text{He}(3^1P)$ with $\text{He}(1^1S)$. The maximum loss rate associated with this process under the conditions of the study is expected to be approximately $7 \times 10^5 \text{ sec}^{-1}$ at 40 mTorr. This should be compared with the experimentally determined loss rate of $1.7 \times 10^7 \text{ sec}^{-1}$ at the same pressure. Hence, collisions were expected to affect the $\tau(3^1P)$ measurements by $\leq 4\%$. For the sake of completeness, a "collision term" was included in the treatment of $\tau(3^1P)$.

Results obtained for the $\tau(3^1P)$ determinations are shown in Fig. 2. The solid line through the data points reflects a "best-fit curve" based on an effective imprisonment radius of $\rho_{\text{eff}} = 1.60 \text{ cm}$. An expansion of the lower-pressure region is used to illustrate the sensitivity of the model to approximately $\pm 10\%$ variations in ρ_{eff} . The

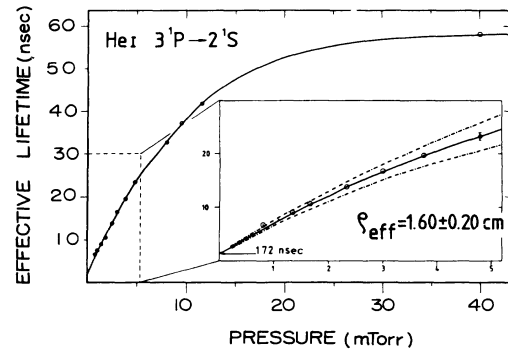


FIG. 2. Results for the pressure-dependent lifetime of $\text{He}(3^1P)$. The solid curve represents the best-fit model for the imprisoned lifetime. The expansion of the low-pressure region illustrates the sensitivity of the calculations to small changes in the value assumed for the effective imprisonment radius ρ_{eff} .

high precision of the lifetime results establishes ρ_{eff} to an estimated $\pm 5\%$. The effective imprisonment radius depends only upon the fixed geometry of the collision chamber as long as the primary source distribution (beam geometry) does not change. Hence, it is reasonable to assume that ρ_{eff} may be used in the evaluation of imprisonment effects for the higher n^1P levels.

C. Collisional angular momentum mixing

It was observed that the decay curves for the higher n^1P levels became complex when the excitation pulse width and the measurement interval were extended into the microsecond domain. For example, the decay of $\text{He}(10^1P)$ at a pressure of 35 mTorr is presented in Fig. 3. Background counts, based on the information in channels 80–100, have been removed from the raw data in preparing the figure. Two points regarding the data in Fig. 3 appear especially significant: (1) the decay curve is obviously complex, and (2) the latter portion of the decay is closely simple exponential with an effective "lifetime" of $4.0 \pm 0.2 \mu\text{sec}$. As previously discussed, cascade effects should be very small for the high n^1P terms under the conditions of our experiment. If one accepts this premise,

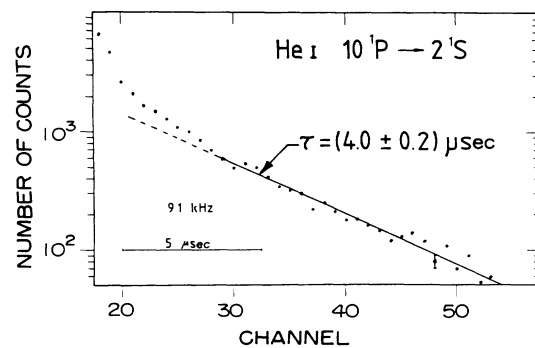


FIG. 3. Decay curve for $\text{He}(10^1P)$ illustrating the prominent, slowly decaying tail observed under conditions such that $\tau_{\text{pulse}} \sim \tau_{\text{tail}}$.

then collisional effects must account for the prominent, slowly decaying tail.

Recent studies of collisional l mixing of Rydberg states in Na and Rb provide insight into the probable source of the slow decay. Gallagher *et al.*¹⁹ observed that collisions between Na(nd) and selected rare-gas collision partners resulted in mixing of the nd state with the $l > 2$ states of the same n . At rare-gas pressures of ~ 1 Torr, the collisional-mixing process was complete, and the observed decay became simple with an effective lifetime equal to the average radiative lifetime of all the collisionally mixed states. The average (or effective) radiative lifetime of the collisionally mixed states was studied for values of n in the range $5 \leq n \leq 15$. An effective lifetime $\tau_{\text{eff}} = 3.68 \pm 0.27 \mu\text{sec}$ was obtained at $n = 10$.

The similarity of the Na($10d$) effective lifetime and the slow component in the case of the He(10^1P) decay suggests collisional l mixing as the mechanism responsible for this behavior. We were unable to conveniently check the decay characteristics of He(10^1P) at significantly higher pressures. However, data taken at a significantly lower pressure (15 mTorr) revealed a decrease in the contribution of the slow component but essentially no change in the decay time of this component. This result is in accord with the model for the l -mixing process. Bagaev *et al.*³⁸ concluded from studies of the decay curves of HeI excited states with $n = 5, 6,$ and 7 that the appearance of anomalously long-lived components signaled the presence of collisionally mixed higher- l states, in accord with the interpretation of the present results.

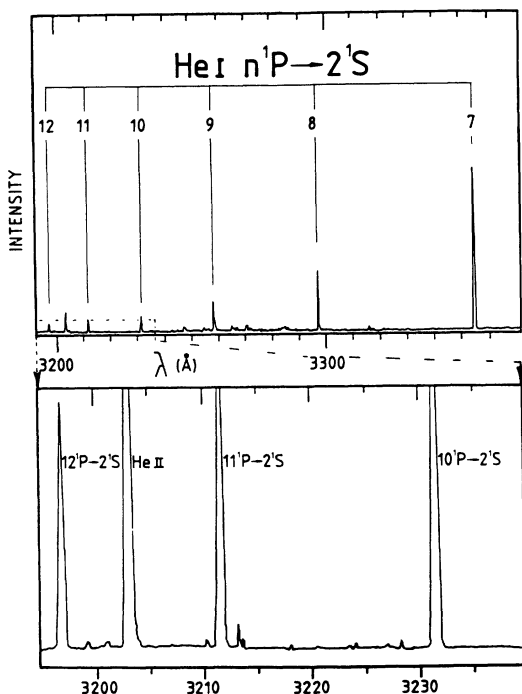


FIG. 4. Spectra produced by 20-keV electrons incident on a He(1^1S) target ($p = 4 \times 10^{-2}$ Torr). The spectra illustrate the prominence of the higher members of the $n^1P \rightarrow 2^1S$ series under these conditions.

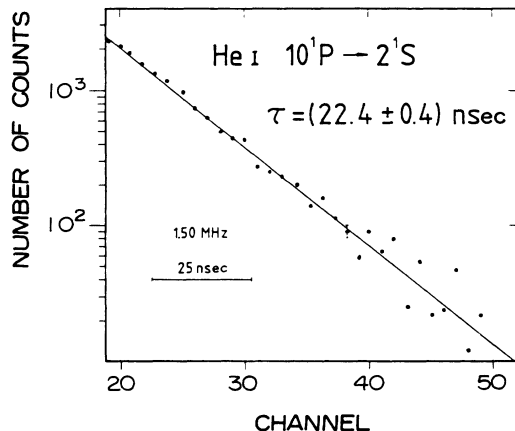


FIG. 5. Decay curve for He(10^1P) illustrating the simple exponential decay observed when the excitation period was short compared to the effective lifetime.

IV. RESULTS AND DISCUSSION

In this section, we first present the essential features of the experimental measurements and then illustrate the method of extracting the information of interest from the data. Results are subsequently compared with previous measurements and, to the extent possible, with pertinent theoretical predictions. Finally, the implications of the results for long-standing problems relating to the interpretation of excitation transfer in gas-kinetic collisions between H(n^1P) and He(1^1S) are discussed.

A. Measurements and data reduction

The spectra in Fig. 4 illustrate the favorable conditions for studying the higher- n members of the HeI $n^1P \rightarrow 2^1S$ series. A large signal-to-background ratio, evident in the lower panel, permitted the acquisition of high-quality lifetime data at target pressures as low as $\sim 10^{-3}$ Torr. The resolution used in obtaining the spectra was $\approx 0.6 \text{ \AA}$, a value typical of that used in the lifetime determinations. Background spectra were essentially negligible under the measurement conditions except for the $9^1P \rightarrow 2^1S$ region where weak $\text{CO}_2^+ A^2\Pi_u \rightarrow X^2\Pi_g$ emissions extended through the position of the line.

Decay-rate determinations were carried out on spectrally selected transitions using the HFD technique. A typical decay curve for the higher- n transitions is presented in Fig. 5 using data for the $10^1P \rightarrow 2^1S$ transition. In contrast with Fig. 3, the decay of He(10^1P) is well described by a single exponential when a short excitation pulse is used. It should be noted that a "constant" background, inferred from the data in channels 60–100, was subtracted from the raw data in preparing Fig. 5. This background presumably originates from random coincidences, very long-lived cascade components, and reciprocal transfer effects. Subtraction of the background consistently yielded single exponentials, indicating negligible time dependence of the background on the time scale of the n^1P measurements.

The only significant difference in the experimental con-

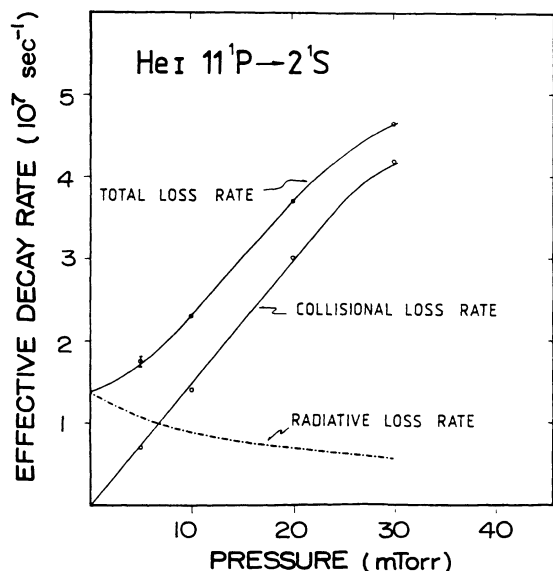


FIG. 6. Effective total decay rate for He(11^1P) vs helium pressure. The inferred contributions from radiative and collisional loss are also shown. The error bar reflects typical statistical uncertainty in the decay-rate determinations.

ditions relating to Figs. 3 and 5 is in the time scale for excitation and observation, which is greater by 2 orders of magnitude in the former case. An explanation of the difference in the decay curves is found within the framework of collisional l mixing. In a first approximation, repopulation effects (reciprocal transfers) become noticeable after a time of the order of the effective lifetime of the repopulating levels.³⁹ The data of Fig. 3 yield an effective lifetime of $\approx 4 \mu\text{sec}$ for the repopulating levels at $n=10$, a value which is much longer than the time scale for the measurements of Fig. 5. Under these short-pulse conditions ($\tau_{\text{pulse}} \ll \tau_{\text{eff}}$), the long-lived higher- L states are significantly underpopulated, and repopulation of the short-lived n^1P levels through reciprocal transfer is negligible.

The method used to extract the collisional loss rate from the total decay rate was sketched in Sec. II. Here we present the results for He(11^1P) to illustrate the method. The set of data points in Fig. 6 defines the total loss rate for He(11^1P) over the pressure range $5 \leq p \leq 30$ mTorr. The contribution of radiative loss as a function of pressure was initially evaluated using the effective imprisonment radius of Fig. 2 and the transition probability data of Wiese *et al.*⁴⁰ The difference between the total loss rate and the radiative loss rate defines the collisional loss rate. Finally, the collisional loss-rate coefficient $\Gamma(11^1P)$ was determined from a least-squares fit to the data in the linear region. The result obtained for $\Gamma(11^1P)$ was $(1.41 \pm 0.29) \times 10^9 \text{ sec}^{-1}/\text{Torr}$, corresponding to an average cross section $\bar{\sigma}(11^1P) = (2.5 \pm 0.6) \times 10^{-13} \text{ cm}^2$. A subsequent, more refined analysis based on a least-squares algorithm for Eqs. (3) and (4) yielded both zero-pressure lifetimes and the final collisional loss-rate coefficients. These results are summarized in Table I.

B. He(n^1P) loss cross sections: Comparison with earlier work

The measured rate constants $\Gamma(n^1P)$, corresponding to the depopulation of He(n^1P) atoms by all collisional processes, are presented in Table I. Related cross sections, $\bar{\sigma}(n^1P)$, derived from the relation (5), are also included in the table together with similar results for $4 \leq n \leq 7$ from earlier investigations. A striking feature of the cross sections summarized in Table I is the exceedingly large spread in the absolute values obtained by various investigators for seemingly the same process. The weight of evidence now points toward collisional l mixing as the probable source of a major portion of this disparity. Recent studies of l mixing have demonstrated that the cross sections for this process can exceed 10^3 \AA^2 under favorable conditions.^{18,19} In sharp contrast, essentially irreversible processes which destroy the excited He(n^1P) atoms under typical experimental conditions are characterized by much smaller cross sections. For example, the associative ioni-

TABLE I. Measured rate coefficients $\Gamma(n^1P)$, in units of $10^8 \text{ sec}^{-1}/\text{Torr}$, and the corresponding average cross sections $\bar{\sigma}(n^1P)$, in units of 10^{-14} cm^2 , for the collisional loss of He(n^1P) in thermal collisions with He(1^1S). The numbers in parentheses represent the experimental uncertainties.

n	$\Gamma(n^1P)$	$\bar{\sigma}(n^1P)$	$\bar{\sigma}(n^1P)$ from other investigations
4	1.13(0.23)	1.98(0.44)	0.028 (Ref. 5), 2.0(0.2) (Ref. 8), 2.3(0.6) (Ref. 9), 2.5(0.2) (Ref. 10), 0.104(0.006) (Ref. 11), 0.20(0.02) (Ref. 12), 2.1(0.2) (Ref. 14), 0.63(0.09) (Ref. 15)
5	2.65(0.53)	4.64(1.07)	6.4(0.7) (Ref. 8), 7.2(0.7) (Ref. 10), 0.104(0.03) (Ref. 11), 5.8(0.6) (Ref. 14)
6	5.18(1.04)	9.06(2.08)	13(3) (Ref. 8), 12(1.5) (Ref. 10), 0.050(0.025) (Ref. 12), 11(1) (Ref. 14)
7	8.34(1.67)	14.6(3.4)	19(3) (Ref. 10), 0.34(0.03) (Ref. 12), 0.023(0.010) (Ref. 11)
8	12.5(2.5)	21.8(5.0)	
9	14.2(2.8)	24.9(5.7)	
10	14.7(2.9)	25.8(5.9)	
11	14.4(2.9)	25.2(5.8)	
12	11.5(2.3)	20.1(4.6)	
13	9.65(1.93)	16.9(3.9)	

TABLE II. Relative cross sections for the collisional loss of $\text{He}(n^1P)$ in thermal collisions with $\text{He}(1^1S)$.

n	This study	Ref. 8	$\bar{\sigma}(n^1P)/\bar{\sigma}(4^1P)$			$\sigma \propto n^4$
			Ref. 10	Ref. 11	Ref. 12	
4	1	1	1	1	1	1
5	2.3	3.2	2.9	1		2.44
6	4.6	6.5	4.8		0.25	5.06
7	7.4		7.6	0.22	1.7	9.38
8	11.0					16.0
9	12.6					25.6
10	13.0					39.1
11	12.7					57.2
12	10.2					81.0
13	8.5					112

zation cross sections for excited-He—normal-He collisions at 300 K are $\leq 10 \text{ \AA}^2$.^{6,15} Under conditions where the l -mixing process does not contribute, the pressure dependence of the effective lifetime of an excited state will be controlled by these situationally irreversible processes, thus yielding significantly reduced effective depopulation cross sections. The spread in the reported results is consistent with this idea.

In Table II, we compare the relative cross sections from the present investigation with similar results from earlier studies. Our relative cross sections are in excellent agreement with those of Wine and Glick,¹⁰ except for $n=5$, and in fair agreement with those of Kay and Hughes.⁸ The results of Bennett *et al.*¹¹ and Bridgett *et al.*¹² are incompatible with the other results in the table. The source of this disparity is not clear but may relate to the initial population distributions obtained in their decay-rate experiments through the use of near-threshold electron-impact excitation. The present results clearly show that the total loss cross sections associated with process (1) vary approximately as n^4 only over the limited range $4 \leq n \leq 6$. When normalized at $n=4$, an n^4 dependence yields overestimations by $\approx 30\%$ at $n=7$ and 300% at $n=10$.

C. Asymptotic behavior of the cross sections

Theoretical studies by Hickman^{23,31} suggest that the $\text{He}(n^1P)$ - $\text{He}(n^1S)$ l -mixing cross sections should vary approximately as $n^{-2.7}$ in the asymptotic region, as indicated in Fig. 8. Our results are in close agreement with this prediction, but the asymptotic behavior is not accurately defined by our measurements, primarily as a result of the paucity of data beyond the peak.

Schiavone *et al.*⁴¹ have deduced effective l -mixing cross sections of $\sim 10^{-14} \text{ cm}^2$ in the case of thermal collisions between high Rydberg and ground-state helium atoms. Their results were not n or l specific, but principal-quantum-number distributions were determined using selective field ionization of the high Rydberg atoms. An effective l -mixing cross section of $200_{-100}^{+200} \text{ \AA}^2$ was obtained in the case of a distribution characterized by a median principal quantum number of $\bar{n}=28$. This result is not l specific, but previously cited theoretical studies in-

dicate that the l -mixing cross sections should depend weakly on the initial l value when the l manifold is effectively degenerate. Hence, it is of interest to compare our lower- n , initial- l -specific measurements with the higher- n results of Schiavone *et al.*⁴¹ Extrapolation of our $n=13$ result to $n=28$ through the use of the theoretically predicted $n^{-2.7}$ asymptotic decline yields about 210 \AA^2 , in remarkable (and probably fortuitous) agreement with the higher- n result. This comparison provides experimental evidence for the general validity of the asymptotic form of the theoretical l -mixing cross sections.

D. Comparison of $\bar{\sigma}(n^1P)$ with $R(n,l) + \text{He}$ l -mixing cross sections

Cross sections obtained in the present investigation exhibit the following salient features: (1) increase closely in proportion to n^4 for $4 \leq n \leq 6$; (2) reach a maximum of $(2.6 \pm 0.6) \times 10^{-13} \text{ cm}^2$ at about $n=10$; and (3) decrease roughly in proportion to $n^{-2.5}$ beyond the peak. These results are quite similar to those of Gallagher *et al.*¹⁹ for the total loss (interpreted as l changing) of $\text{Na}(n^2D)$ ($6 \leq n \leq 15$) in thermal collisions with $\text{He}(1^1S)$, both with regard to the n dependence of the loss and the magnitude of the cross sections. Hugon *et al.*¹⁸ have also reported

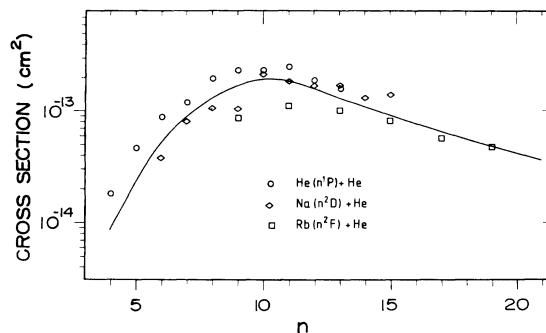


FIG. 7. Comparison of loss cross sections vs n for thermal collisions of $\text{He}(n^1P)$, $\text{Na}(n^2D)$, and $\text{Rb}(n^2F)$ with $\text{He}(1^1S)$. The curve reflects predictions based on a scaling formula for l -changing cross sections associated with the $\text{Na}(n^2D)$ - $\text{He}(1^1S)$ collisions.

similar results in the case of thermal collisions of $\text{Rb}(n^2F)$ ($9 \leq n \leq 21$) with $\text{He}(1^1S)$.

The similarity of the results in these three cases is illustrated in Fig. 7. A curve based on the application of the previously mentioned l -mixing scaling formula³¹ to the $\text{Na}(n^2D) + \text{He}$ collisions is seen to agree well with the experimental results. This formula is not directly applicable to the $\text{He}(n^1P) + \text{He}$ and $\text{Rb}(n^2F) + \text{He}$ collisions since it was derived assuming that the initial level was characterized by $l=2$. An approximate modification required for a valid comparison of the scaling-formula predictions with the $\text{He}(n^1P)$ and $\text{Rb}(n^2F)$ results will subsequently be discussed. For present purposes, it suffices to note that the scaling formula yields nearly identical results for the three cases when $n \geq 10$, in agreement with the observations.

The comparisons in Fig. 7 strongly suggest that the dominant loss process for the excited atoms in each of the three experiments was collisional l changing. Indeed, Gallagher *et al.*¹⁹ convincingly demonstrated the dominance of this process in their experiment by investigating the decay of $\text{Na}(n^2D)$ over a wide range of He concentrations. At He pressures ~ 1 Torr, the l -mixing process was found to be complete, and the $\text{Na}(n^2D)$ decayed at an effective rate in agreement with the theoretical average rate for collisionally mixed levels. Higgs *et al.*⁴² similarly determined that collisional l mixing was the only detectable depopulation mechanism in their study of the destruction of $\text{Xe}(nf)$ Rydberg atoms by thermal collisions with Xe, Kr, Ar, CO_2 , CO, and N_2 .

E. Comparisons with theoretical treatments of l mixing

It is of interest to consider our results within the framework of recent theoretical treatments of l -changing collisions. In this connection, we note that a completely satisfactory theory of transitions between Rydberg states induced in thermal atom-atom collisions does not exist in the case of the intermediate range of principal quantum numbers ($5 \leq n \leq 15$) pertinent to the present experiment. In this domain of n , the velocity of the Rydberg electron greatly exceeds the relative velocity in the atom-atom collision at 300 K. Hence, a complete theoretical treatment should be based on a molecular approach rather than on the widely adopted separated-atom model. As previously noted, Cohen³⁰ has applied a molecular model in treating excitation transfer in thermal $\text{He}(1^1S)$ - $\text{He}(3^3L)$ collisions, but apparently no attempt has been made to extend these calculations beyond $n=3$. We are unaware of other molecular treatments of the He-He* collision problem at thermal energies.

Most of the recent simple theoretical descriptions of l -changing thermal collisions are based on an impulse-type treatment of the Rydberg electron-perturber interaction and neglect the so-called "noninertiality" of the core. Flannery²⁶ has noted that these theoretical treatments do not address certain "impulse-validity criteria" and tend to yield results which significantly exceed the upper limit imposed by the basic impulse expression. He also notes that these treatments entail the use of further computational simplifications within the basic impulse expression, a situation which necessitates additional validity criteria.

In addition, he suggests that the role of the core in the thermal l -changing collisions is sufficiently unclear as to warrant a detailed theoretical study based on a full molecular approach. Several recent papers have been directed toward clarification of these issues and toward the identification of model deficiencies.^{26-29,44}

Despite model limitations, considerable progress has been made in theoretically describing the qualitative features of the quasielastic l -mixing collisions involving selected Rydberg atoms and a number of collision partners. In this connection, an approximate scaling formula has been developed³¹ which allows the rapid estimation of l -mixing cross sections associated with Rydberg atom-perturber collisions at thermal energies. The scaling formula has now been applied to numerous test cases and has consistently reproduced the overall n dependence of the measured cross sections, while only qualitatively reproducing the absolute values (typically to within a factor of 2).

Prior to comparing the predictions of the scaling relationship with our measurements, it is of interest to consider upper bounds for the l -changing process as provided within the framework of the impulse approximation. It has been shown⁴³ that the l -changing cross sections due solely to Rydberg electron-perturber collisions should be approximately equal to or less than the "average cross section" for elastic scattering of free electrons having the same velocity distribution as the Rydberg electron. This "upper-limit" cross section $\bar{\sigma}_u$ may be written in the form

$$\bar{\sigma}_u \lesssim (1/\bar{v}) \int v_e \sigma(v_e) f(v_e) dv_e, \quad (7)$$

where \bar{v} is the mean relative collision velocity of the Rydberg atom and the target, $f(v_e)$ is the velocity distribution function for the Rydberg electron, and $\sigma(v_e)$ is the free-electron elastic-scattering cross section.

In the case of low-energy-electron scattering by He, the cross section is weakly dependent on energy and remains nearly constant over the range of velocities associated with a Rydberg electron. Hence, the integral may be approximated by the product $\bar{v}_e \sigma(\bar{v}_e)$, where \bar{v}_e is the average velocity of the electron. The expression (7) then takes the simple form

$$\bar{\sigma}_u \lesssim \frac{\bar{v}_e \sigma(\bar{v}_e)}{\bar{v}}. \quad (8)$$

Let us compare the upper limit from (8) with the data in the case $n=10$, which corresponds to the peak experimental cross section. This value of n is sufficiently large to justify the use of many of the "large- n approximations," as previously noted. The ratio (\bar{v}_e/\bar{v}) is then about 1.2×10^2 and $\sigma(\bar{v}_e) \cong 5.6 \times 10^{-16} \text{ cm}^2$, yielding a value $6.7 \times 10^{-14} \text{ cm}^2$ for the upper-bound cross section at $n=10$. The experimental result in Table I [$(2.6 \pm 0.6) \times 10^{-13} \text{ cm}^2$] exceeds the impulse upper limit by a factor of 3.9. Inclusion of an upper limit for inelastic transitions associated with the core-perturber interaction⁴² increases the upper limit to $\approx 10^{-13} \text{ cm}^2$, a value which is still significantly smaller than the measured value. Flannery²⁶ has noted that the impulse upper limit [Eq. (7)] consistently yields values much lower than experiment,

especially for the lighter targets, and has suggested that the inclusion of an upper bound for core effects leads to limits which are much more consistent with the measured cross sections. However, in the present case of He-He* collisions at 300 K, it is clear that inclusion of the suggested upper bound for core effects does not substantially improve the agreement with the experimental result. The explanation of this discrepancy is unclear at this juncture but may stem from the approximate nature of the upper limit.^{43,44}

Let us now turn to a comparison of the experimental results with the recently published approximate scaling relationship for estimating l -mixing cross sections. Following Hickman,³¹ the scaling relationship may be written in the form

$$\sigma_{l\text{mix}} = [n^4 f(\gamma) g(\beta)] (\pi a_0^2), \quad (9)$$

where $f(\gamma)$ and $g(\beta)$ are empirically derived functions based on limited quantum-theoretical results. The function $f(\gamma)$, termed the collision efficiency, decreases monotonically with increasing values of the reduced parameter γ which is defined by

$$\gamma \equiv \frac{2\pi n^2 a_0 \Delta E}{h\bar{v}}, \quad (10)$$

with ΔE the "energy defect" for the collision and \bar{v} the mean relative collision speed. The other symbols have the usual meanings. The function $g(\beta)$, termed the probability of encounter, increases with increasing β toward an arbitrarily set asymptotic value of 0.6 for $\beta \geq 3.0$. The reduced parameter β is defined by

$$\beta \equiv \frac{(hA/2\pi m_e a_0^2)}{(\bar{v}n^{3.367})}, \quad (11)$$

where $A \rightarrow L$ (the scattering length) for large n .

In order to apply Eq. (9) to the present problem, some assumptions are required. The pertinent assumptions are: (1) there is no selection rule for the l -changing transitions; (2) the $\Delta E (nD - nF)$ separations in He I are small enough to justify quasidegeneracy; (3) A in Eq. (12) is adequately represented by L for the range of n under consideration. In the present experiment, the initial level had $l=1$ rather than $l=2$, the value assumed in deriving the scaling relationship. The accessible final states are taken to be the quasidegenerate set $l=2, 3, \dots, n-1$. (The state with $l=0$ is neglected because of the relatively large energy gap separating this state from the $l \geq 1$ states.) When electron spin is neglected, the number of accessible final states is n^2-4 . This compares with the number n^2-9 which was used in the development of the scaling relationship. Assumption (1), which is reasonably well supported by both theory and experiment, enables one to write

$$\sigma_{l\text{mix}}(np) = \frac{(n^2-4)}{(n^2-9)} \sigma_{l\text{mix}}(nd). \quad (12)$$

We have used this simple adjustment of Eq. (9) in computing cross sections to compare with the data of Table I.

These computations are summarized in Fig. 8, where they are compared with the measurements. (The values

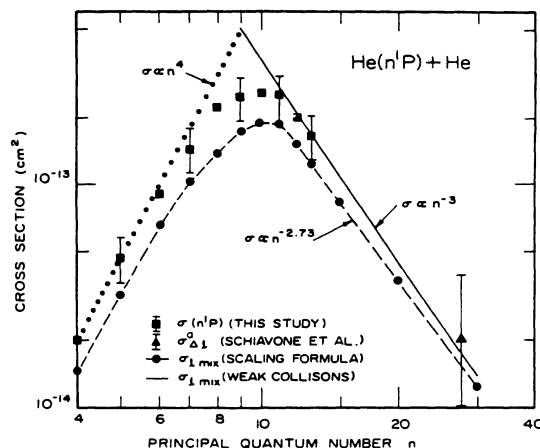


FIG. 8. Log-log presentation of the He(n^1P) collisional loss cross sections illustrating the n^4 behavior at low n and the trend toward an $\sim n^{-2.5}$ variation beyond the peak. Predictions based on a modified scaling relationship for l -changing collisions are shown by dots connected with a broken line. The results of a perturbative treatment of l -changing collisions in the weak-collision approximation are represented by the solid line. The cited works are as follows: Schiavone *et al.*, Ref. 41; scaling formula, Ref. 31; and weak collisions, Ref. 32.

for ΔE were taken from Martin⁴⁵ to $n=20$ and extrapolated to higher n by means of an n^{-3} scaling. A value 1.8×10^5 cm sec⁻¹ was used for the mean relative collision velocity.) Cross sections computed from the modified scaling relationship are uniformly about 0.7 of the measured values, which is within the estimated accuracy³¹ of the scaling relationship. We also note from Fig. 8 that a simple perturbative treatment of the l -mixing problem in the weak-collision approximation³² has yielded results for $n \geq 11$ which are in excellent agreement with the measured values. The scattering-length approximation and JWKB wave functions were used in these calculations, and it was assumed that transitions with $\Delta n \neq 0$ could be neglected. A simple formula for collisional l mixing resulted, i.e.,

$$\sigma_{l\text{mix}} = (2\pi L^2) / (n^3 \bar{v}^2). \quad (13)$$

This expression yields cross sections for $n \geq 11$ which are in satisfactory accord with those obtained from the scaling relationship.

F. Implications for excitation transfer in He(n^1P)-He collisions

It is of interest to consider the implications of the present results for the general problem of possible ΔL selection rules associated with thermal He(n^1P)-He collisions. Interest in this problem dates to the theoretical study of Lin and Fowler⁴⁶ from which it was concluded that transfers with $\Delta L=0, \pm 2$ should be favored in He-He* collisions at thermal energies. Several subsequent treatments of He(n^1P) collisional loss tended to support the $P \rightarrow F$ transfer mechanism, but a growing body of relevant data and theoretical computations have cast considerable doubt on the degree of ΔL selectivity involved in

the transfer of excitation. Indeed, the singlet-triplet anticrossing studies of Freund *et al.*⁴⁷ provide direct evidence for violations of the $\Delta L = \pm 2$ selection rule.

Decay-rate data of the type shown in Fig. 3 provide information of value to the problem of ΔL selectivity in the collisions. In the case of reciprocal excitation transfer between two collisionally coupled levels, the decay of each level is described by a sum of two exponential terms. The inclusion of more than two states in the process merely increases the number of exponential components required to describe the decay of each level. In the absence of cascade, a multiexponential decay would imply strong ΔL selection rules in the collisions. In sharp contrast, the absence of ΔL selection rules for the collisions should result in only two exponential components in the time-resolved decay of a single level which was initially populated in a selective manner.¹⁹ In the absence of ΔL selection rules, the transfer of population to the adjacent levels is statistically distributed under single-collision condition. Hence, the "mixture" of adjacent states decays at a rate corresponding to the statistically averaged radiative value for the ensemble while the decay of the initially occupied level reflects both radiative decay and collisional transfers. The transfer of excitation is, of course, initially unidirectional, but reciprocal transfers become increasingly important as the populations of the adjacent levels grow.

In the present experiment, it was observed that the decay of $\text{He}(n^1P)$ was not adequately described by one or two exponential components under certain experimental conditions. For example, the decay curve in Fig. 3 requires a minimum of three components for an adequate description. Bagaev *et al.*³⁸ have similarly found that several exponential components were required to describe the decay of $\text{He}(n^1P)$ levels with $n = 5-7$ under their experimental conditions. Hence, it would appear that the $\text{He}(n^1P)$ -He data demand some degree of selectivity in the ΔL for the collisional mixing process, at least for the levels with $n \leq 10$. The behavior of the longest-lived portion of the $\text{He}(10^1P)$ decay is consistent with collisionally mixed states with $L \geq 3$, in accord with the lower- n measurements of Bagaev *et al.*³⁸ These results suggest the need for more refined studies to investigate the final-state L distribution for collisions of type (1) under single-collision conditions.

Although the present observations do not yield a final answer to the question of ΔL selection rules for the thermal $\text{He}(n^1P)$ -He collisions, the prominent, slowly decaying tails on the $\text{He}(n^1P)$ decay curves, under conditions such that $\tau_{\text{pulse}} > \tau_{\text{eff}}$, are most satisfactorily interpreted in terms of essentially unrestricted collisional mixing of the n^1P level under study with adjacent L levels (same n).

For example, the late-time decay of $\text{He}(10^1P)$ in Fig. 3 is well characterized by a "lifetime" of about $4 \mu\text{sec}$. This component contributes roughly 25% to the early-time decay, a value greatly in excess of that expected for radiative transfer from levels with $n > 10$ (see Sec. III A). Collisional mixing of $\text{He}(10^1P)$ with the adjacent $10L$ levels is expected to yield a slow component characterized by a lifetime of about $2.7 \mu\text{sec}$ if the mixing is with the $L \geq 2$ lev-

els and about $3.4 \mu\text{sec}$ if the mixing is restricted to levels with $L \geq 3$, as suggested by Bagaev *et al.*³⁸ The experimental τ_{eff} exceeds both of these values, but the disparity between τ_{eff} and the longer statistically averaged lifetime is deemed insignificant. Interpretational uncertainties stemming from the possibilities of a small contribution from long-lived cascade components and modest collisional n mixing with $n = 11$ (Ref. 48) do not permit us to unequivocally choose between the alternatives $L \geq 2$ and $L \geq 3$.

These results support the conclusion of Freund *et al.*⁴⁷ that transfers with $\Delta L = \pm 2$ are not favored in the He-He* collisions. For example, the upper limit expected for τ_{eff} in Fig. 3 if the $10^1P \leftrightarrow 10F$ process were dominant is about $1.1 \mu\text{sec}$, in disagreement with the observations. However, the assumption of unrestricted collisional mixing of $\text{He}(10^1P)$ with the $10L$ -singlets ($L \geq 3$) is consistent with the observations, as noted above. When combined with the complementary results of Bagaev *et al.*³⁸ and those of Freund *et al.*,⁴⁷ the present observations suggest the need for reinterpretation of the results from earlier studies in which a selective $n^1P \leftrightarrow nF$ collisional process was assumed in interpreting steady-state and time-resolved studies of excitation transfer in helium.

V. SUMMARY AND CONCLUSIONS

Determinations of total loss cross sections for $\text{He}(n^1P)$ in collisions with $\text{He}(1^1S)$ at 300 K have been made for a range of intermediate principal quantum numbers ($4 \leq n \leq 13$). These results significantly extend previous measurements and provide valuable insight into the dominant loss mechanism. The cross sections increase closely in proportion to the geometric cross section over the limited range $4 \leq n \leq 6$, reach a maximum of about $2.6 \times 10^3 \text{ \AA}^2$ at $n = 10$, and decrease roughly as $n^{-2.5}$ above the peak. These results are consistent with collisional l mixing as the dominant quenching mechanism, in accord with a number of recent investigations of the collisional destruction of Rydberg atoms in thermal collisions with various perturbers. In particular, the $\text{He}(n^1P)$ -He loss cross sections are nearly identical to those associated with thermal $\text{Na}(n^2D)$ -He and $\text{Rb}(n^2F)$ -He collisions when $n \geq 10$, a result which suggests that the Rydberg core plays a minor role in l -changing collisions of this type.

It was found that a scaling relationship for l -changing collisions, modified for the number of accessible final states, yielded cross sections which were about 0.7 of the experimental values over the full range of n . An approximate expression for cross sections of quasielastic collisions ($\Delta n = 0$) for intermediate n values ($n \sim 15-20$), based on a perturbative treatment of weak collisions in the scattering-length approximation with JWKB wave functions, yields results which are in excellent agreement with the measurements when $n \geq 11$.

Finally, we note that the measurements were found to be inconsistent with a strong "selection rule" $\Delta L = 2$ for the $\text{He}(n^1P)$ -He collisions, in agreement with evidence from other independent experiments. Rather, a model in which the change in L during the collision is largely unre-

stricted provides a much better interpretation of the observations.

ACKNOWLEDGMENTS

The authors are grateful to Professor Peter Erman and to Professor Georg Witt for their interest in this study and for helpful input relating to certain aspects of collisional

energy transfer in atomic collisions. On of us (W.R.P.) would like to express his appreciation to the Swedish Natural Science Research Council and to the Division of Research at Utah State University for providing funds towards his stay in Sweden. Also, the hospitality of the Research Institute of Physics and of the Meteorological Institute of the University of Stockholm is gratefully acknowledged by W.R.P.

-
- *Permanent address: Department of Physics, Utah State University, Logan, UT 84322.
- ¹J. H. Lees and H. W. B. Skinner, Proc. R. Soc. London, Ser. A **137**, 186 (1932).
 - ²W. Maurer and R. Wolf, Z. Phys. **92**, 100 (1934).
 - ³R. Wolf and W. Maurer, Z. Phys. **115**, 410 (1940).
 - ⁴A. H. Gabriel and D. W. O. Heddle, Proc. R. Soc. London, Ser. A **258**, 124 (1960).
 - ⁵J. Bakos and J. Szigeti, J. Phys. B **1**, 1115 (1968).
 - ⁶H. F. Wellenstein and W. W. Robertson, J. Chem. Phys. **56**, 1411 (1972).
 - ⁷A. F. J. van Raan and J. van Eck, J. Phys. B **7**, 2003 (1974).
 - ⁸R. B. Kay and R. H. Hughes, Phys. Rev. **154**, 61 (1967).
 - ⁹J. D. Jobe and R. M. St. John, Phys. Rev. A **5**, 295 (1972).
 - ¹⁰P. H. Wine and R. E. Glick, J. Quant. Spectrosc. Radiat. Transfer **16**, 879 (1976).
 - ¹¹W. R. Bennett, Jr., P. J. Kindlmann, and G. N. Mercer, Appl. Opt. Suppl. **2**, 34 (1965).
 - ¹²K. A. Bridgett, T. A. King, and R. J. Smith-Saville, J. Phys. E **3**, 767 (1970).
 - ¹³W. W. Hunter, Jr. and T. E. Leinhardt, J. Chem. Phys. **58**, 941 (1973).
 - ¹⁴D. E. Lott III, R. E. Glick, and J. A. Llewellyn, J. Quant. Spectrosc. Radiat. Transfer **15**, 513 (1975).
 - ¹⁵A. Catherinot and B. Dubreuil, Phys. Rev. A **23**, 763 (1981).
 - ¹⁶P. Erman, Phys. Scr. **11**, 65 (1975).
 - ¹⁷T. F. O'Malley, Phys. Rev. **130**, 1020 (1963).
 - ¹⁸M. Hugon, F. Gounand, P. R. Fournier, and J. Berlande, J. Phys. B **12**, 2707 (1979).
 - ¹⁹T. F. Gallagher, S. A. Edelstein, and R. M. Hill, Phys. Rev. A **15**, 1945 (1977).
 - ²⁰J. I. Gersten, Phys. Rev. A **14**, 1354 (1976).
 - ²¹T. Derouard and M. Lombardi, J. Phys. B **11**, 3875 (1978).
 - ²²A. P. Hickman, Phys. Rev. A **18**, 1339 (1978).
 - ²³A. P. Hickman, Phys. Rev. A **19**, 994 (1979).
 - ²⁴E. de Prunele and J. Pascale, J. Phys. B **12**, 2411 (1979).
 - ²⁵V. A. Smirnov, Opt. Spektrosk. **37**, 407 (1974) [Opt. Spectrosc. (U.S.S.R.) **37**, 231 (1974)].
 - ²⁶M. R. Flannery, J. Phys. B **13**, L657 (1980).
 - ²⁷Y. Hahn, J. Phys. B **15**, 613 (1982).
 - ²⁸A. P. Hickman, J. Phys. B **14**, L419 (1981).
 - ²⁹M. Matsuzawa, J. Phys. B **14**, L553 (1981).
 - ³⁰J. S. Cohen, Phys. Rev. A **13**, 86 (1976).
 - ³¹A. P. Hickman, Phys. Rev. A **23**, 87 (1981).
 - ³²A. Omont, J. Phys. (Paris) **39**, 1343 (1977).
 - ³³P. Erman and J. Brzozowski, Phys. Scr. **12**, 177 (1975).
 - ³⁴R. M. St. John, F. L. Miller, and C. C. Lin, Phys. Rev. **134**, A888 (1964).
 - ³⁵A. V. Phelps, Phys. Rev. **110**, 1362 (1958).
 - ³⁶T. Holstein, Phys. Rev. **72**, 1212 (1947); **83**, 1159 (1951).
 - ³⁷F. E. Irons, J. Quant. Spectrosc. Radiat. Transfer **22**, 21 (1979).
 - ³⁸S. A. Bagaev, O. V. Oginets, V. B. Smirnov, and Yu. A. Tolmachev, Opt. Spektrosk. **46**, 1067 (1949) [Opt. Spectrosc. (U.S.S.R.) **46**, 603 (1979)].
 - ³⁹F. Gounand, P. R. Fournier, and J. Berlande, Phys. Rev. A **15**, 2212 (1977).
 - ⁴⁰W. L. Wiese, M. W. Smith, and B. M. Glennon, Natl. Stand. Ref. Data Ser., U.S. Natl. Bur. Stand. NSRDS-NBS-4, 1966 (unpublished).
 - ⁴¹J. A. Schiavone, D. E. Donohue, D. R. Herrick, and R. S. Freund, Phys. Rev. A **16**, 48 (1977).
 - ⁴²C. Higgs, K. A. Smith, F. B. Dunning, and R. F. Stebbings, J. Chem. Phys. **75**, 745 (1981).
 - ⁴³M. R. Flannery, Phys. Rev. A **22**, 2408 (1980).
 - ⁴⁴M. R. Flannery, J. Phys. B **15**, 3249 (1982).
 - ⁴⁵W. C. Martin, J. Res. Natl. Bur. Stand. **64**, 19 (1960).
 - ⁴⁶C. C. Lin and R. G. Fowler, Ann. Phys. (N.Y.) **15**, 461 (1961).
 - ⁴⁷R. S. Freund, T. A. Miller, B. R. Zegarski, R. Jost, M. Lombardi, and A. Dorelon, Chem. Phys. Lett. **51**, 18 (1977).
 - ⁴⁸F. Devos, J. Boulmer, and J.-F. Delpech, J. Phys. (Paris) **40**, 215 (1979).